

Crystal structure of the thalidomide analog (3a*R*^{*},7a*S*^{*})-2-(2,6-dioxopiperidin-3-yl)hexahydro- 1*H*-isoindole-1,3(2*H*)-dione

Yousef Hijji,^a Ellis Benjamin,^b Jerry P. Jasinski^c and Ray J. Butcher^{d*}

Received 23 August 2018

Accepted 10 October 2018

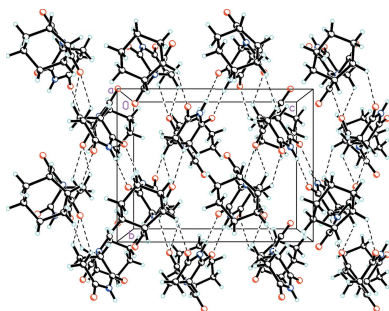
Edited by A. J. Lough, University of Toronto,
Canada**Keywords:** crystal structure; thalidomide
analogs; pseudomeroherdal twinning.**CCDC reference:** 1872551**Supporting information:** this article has
supporting information at journals.iucr.org/e

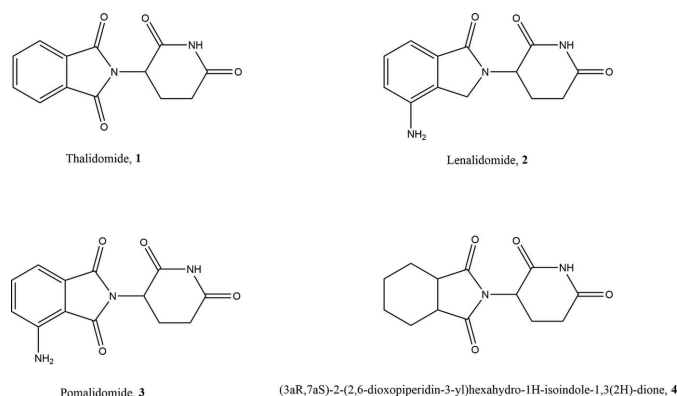
^aDepartment of Chemistry and Earth Sciences, Qatar University, Doha, Qatar, ^bDepartment of Chemistry, Richard Stockton College of New Jersey, Galloway, NJ 08205, USA, ^cDepartment of Chemistry, Keene State College, 229 Main Street, Keene NH 03435, USA, and ^dDepartment of Chemistry, Howard University, 525 College Street NW, Washington, DC 20059, USA. *Correspondence e-mail: rbutcher99@yahoo.com

The title compound, C₁₃H₁₆N₂O₄, crystallizes in the monoclinic centrosymmetric space group, *P*2₁/*c*, with four molecules in the asymmetric unit, thus there is no crystallographically imposed symmetry and it is a racemic mixture. The structure consists of a six-membered unsaturated ring bound to a five-membered pyrrolidine-2,5-dione ring N-bound to a six-membered piperidine-2,6-dione ring and thus has the same basic skeleton as thalidomide, except for the six-membered unsaturated ring substituted for the aromatic ring. In the crystal, the molecules are linked into inversion dimers by *R*₂²(8) hydrogen bonding involving the N—H group. In addition, there are bifurcated C—H···O interactions involving one of the O atoms on the pyrrolidine-2,5-dione with graph-set notation *R*₂¹(5). These interactions along with C—H···O interactions involving one of the O atoms on the piperidine-2,6-dione ring link the molecules into a complex three-dimensional array. There is pseudomeroherdal twinning present which results from a 180° rotation about the [100] reciprocal lattice direction and with a twin law of 1 0 0 0 $\bar{1}$ 0 0 0 $\bar{1}$ [BASF 0.044 (1)].

1. Chemical context

Thalidomide (**1**) is one of the most notorious drugs in pharmaceutical history because of the humanitarian disaster in the 1950s (Burley & Lenz, 1962; Stephans, 1988; Bartlett *et al.*, 2004; Wu *et al.*, 2005; Melchert & List, 2007). Thalidomide possesses a single stereogenic carbon in the glutarimide ring, and it is conceivable that the unexpected teratogenic side effects are ascribed to the (*S*)-enantiomer of **1** (Blaschke *et al.*, 1979). However, this has been a matter of debate because considerable chiral inversion should take place during the incubation of enantiomerically pure **1** (Nishimura *et al.*, 1994; Knoche & Blaschke, 1994; Wnendt *et al.*, 1996). Despite the tragic disaster, the unique biological properties of **1** prompted its return to the market in the 21st century for the treatment of multiple myeloma and leprosy (Matthews & McCoy, 2003; Hashimoto *et al.*, 2004; Franks *et al.*, 2004; Brennen *et al.*, 2004; Luzzio *et al.*, 2004; Sleijfer *et al.*, 2004; Kumar *et al.*, 2004; Hashimoto, 2008; Knobloch & Rüther, 2008). Furthermore, a large number of papers on novel medical uses of **1** continue to appear in the biological and medicinal literature (Matthews & McCoy, 2003; Hashimoto *et al.*, 2004; Franks *et al.*, 2004; Brennen *et al.*, 2004; Luzzio *et al.*, 2004; Sleijfer *et al.*, 2004; Kumar *et al.*, 2004; Hashimoto, 2008; Knobloch & Rüther, 2008).





Thus, over the years, there has been increasing interest in thalidomide and its derivatives for the treatment of various hematologic malignancies (Singhal *et al.*, 1999; Raje & Anderson, 1999), solid tumors (Kumar *et al.*, 2002), and a variety of inflammatory and autoimmune diseases (Tseng *et al.*, 1996). Recent studies have uncovered a variety of mechanisms of thalidomide action. It was reported in 1991 that thalidomide is a selective inhibitor of tumor necrosis factor- α (TNF- α) production in lipopolysaccharide (LPS) stimulated human monocytes (Moreira *et al.*, 1993; Sampaio *et al.*, 1991). TNF- α is a key pro-inflammatory cytokine, and elevated levels have been linked with the pathology of a number of inflammatory and autoimmune diseases including rheumatoid arthritis, Crohn's disease, aphthous ulcers, cachexia, graft *versus* host disease, asthma, ARDS and AIDS (Eigler *et al.*, 1997). Taken together, the immunomodulatory properties of thalidomide, which are dependent on the type of immune cell activated as well as the type of stimulus that the cell receives, provide a rationale for the mechanism of thalidomide action in the context of autoimmune and inflammatory disease states. Other pharmacologic activities of thalidomide include its inhibition of angiogenesis (D'Amato *et al.*, 1994) and its anti-cancer properties (Bartlett *et al.*, 2004). In the late 1990's it was reported that thalidomide is efficacious for the treatment of multiple myeloma (MM), a hematological cancer caused by growth of tumor cells derived from the plasma cells in the bone marrow (Singhal *et al.*, 1999; Raje & Anderson, 1999).

A medicinal chemistry program to optimize the immunomodulatory properties of thalidomide and reduce its side-effects led to the discovery of lenalidomide (2), which is a potent immunomodulator that is ~800 times more potent as an inhibitor of TNF- α in LPS-stimulated hPBMC (Muller *et al.*, 1999; Zeldis *et al.*, 2011). In the US, lenalidomide was approved by the FDA in 2005 for low- or intermediate-1-risk myelodysplastic

Structural optimization of thalidomide, 1 also led to the discovery of pomalidomide (3), which is tenfold more potent than lenalidomide as a TNF- α inhibitor and IL-2 stimulator (Muller *et al.*, 1999; Zeldis *et al.*, 2011). Pomalidomide is currently undergoing late-stage clinical development for the treatment of multiple myeloma and myeloproliferative

neoplasm-associated myelofibrosis (Galustian & Dalglish, 2011; Begna *et al.*, 2012). In clinical trials for multiple myeloma, pomalidomide has been shown to be effective in overcoming resistance to lenalidomide and thalidomide, as well as the proteasome inhibitor bortezomib (Schey & Ramasamy, 2011).

These studies have shown the efficacy of a continued search for more pharmacologically active analogs of thalidomide and its derivatives. Focus has previously been on modifying the basic thalidomide skeleton by changing its substituents. However, there have been very few studies on related derivatives where the six-membered ring is changed from an aromatic to an unsaturated ring. In view of the wide interest in these types of compounds for their pharmacological activities, the structure of (3aR,7aS)-2-(2,6-dioxopiperidin-3-yl)hexahydro-1H-isoindole-1,3(2H)-dione, 4, is reported where the only change to thalidomide is the substitution of an unsaturated six-membered for the aromatic ring.

As a result of this interest in thalidomide, the crystal structure of this molecule in both the racemic and enantiomerically pure forms have been determined multiple times (Lovell, 1970, 1971; Reepmeyer *et al.*, 1994; Allen & Trotter, 1971; Caira *et al.*, 1994; Suzuki *et al.*, 2010; Maeno *et al.*, 2015). Two polymorphs of the racemic derivative have been determined crystallizing in the space groups $P2_1/n$ (Allen & Trotter, 1971; Suzuki *et al.*, 2010; Maeno *et al.*, 2015) and $P2_1/c$ (Lovell, 1970) or $C2/c$ (Reepmeyer *et al.*, 1994; Caira *et al.*, 1994). The crystal packing in the $C2/c$ structure is determined by intermolecular N-H...O hydrogen bonding that is more extensive than that reported for the racemate of thalidomide crystallizing in space group $P2_1/n$.

2. Structural commentary

The title compound, $C_{13}H_{16}N_2O_4$, 4 (Fig. 1), crystallizes in the monoclinic centrosymmetric space group, $P2_1/c$, with four molecules in the asymmetric unit, thus there is no crystallographically imposed symmetry and it is a racemic mixture. The structure consists of a six-membered unsaturated ring bound to a five-membered pyrrolidine-2,5-dione ring N-bound to a six-membered piperidine-2,6-dione ring and thus has the same basic skeleton as thalidomide, 1, except for the six-

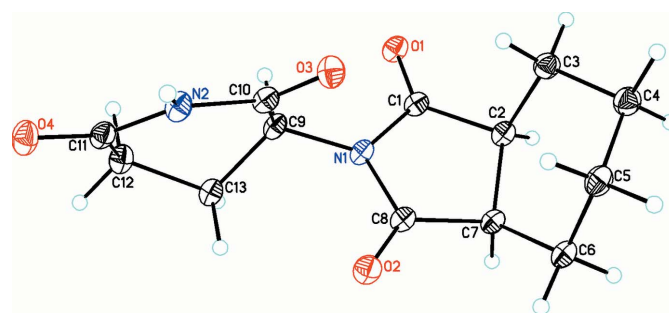


Figure 1
The molecular structure of the title compound 4, with the atom-numbering scheme. Atomic displacement parameters are drawn at the 30% probability level.

Table 1
Hydrogen-bond geometry (Å, °).

$D-H\cdots A$	$D-H$	$H\cdots A$	$D\cdots A$	$D-H\cdots A$
$N2-H2N\cdots O3^i$	0.88 (5)	2.07 (5)	2.928 (3)	165 (4)
$C7-H7A\cdots O4^{ii}$	1.00	2.42	3.150 (3)	129
$C9-H9A\cdots O1^{iii}$	1.00	2.65	3.385 (3)	130
$C12-H12A\cdots O2^{ii}$	0.99	2.53	3.143 (3)	120
$C13-H13A\cdots O2$	0.99	2.56	3.142 (3)	118
$C13-H13B\cdots O2^{ii}$	0.99	2.52	3.163 (3)	122

Symmetry codes: (i) $-x+1, -y+2, -z+1$; (ii) $-x+1, y-\frac{1}{2}, -z+\frac{3}{2}$; (iii) $-x+1, -y+1, -z+1$.

membered unsaturated ring substituted for the aromatic ring. In the five-membered pyrrolidine-2,5-dione ring, the atoms O1, C1, N1, C8 and O2 form a plane (r.m.s. deviation of fitted atoms = 0.0348 Å) with C2 and C7 deviating from this plane by -0.186 (7) and 0.219 (7) Å, respectively. The ring itself adopts a conformation in which it is twisted about the C2–C7 axis [$P = 257.4$ (5) and $\tau = 22.5$ (2); Rao *et al.*, 1981]. In the six-membered piperidine-2,6-dione ring, the group, O3, C10, N2, C11 and O4 is also planar (r.m.s. deviation of fitted atoms = 0.0042 Å). The cyclohexane ring adopts a chair conformation [puckering parameters $Q = 0.536$ (3), $\theta = 157.7$ (3)° and $\varphi = 324.2$ (8)°; Boeyens, 1978). Otherwise, the metrical parameters for all bonds are in the standard range for such structures.

3. Supramolecular features

Similarly to the hydrogen-bonding patterns found in both the enantiomerically pure form of thalidomide (Lovell, 1971; Maeno *et al.*, 2015) and the racemic $P2_1/n$ polymorph (Allen & Trotter, 1971; Suzuki *et al.*, 2010; Maeno *et al.*, 2015), the molecules of the title compound are linked into inversion dimers by $R_2^2(8)$ (Etter *et al.*, 1990) hydrogen bonding (Table 1) involving the N–H group as shown in Fig. 2. In addition, there

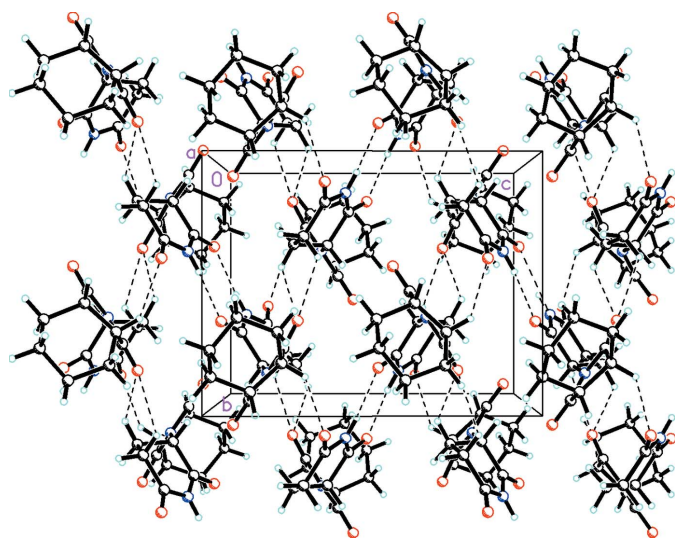


Figure 2
Packing diagram viewed along the a axis showing the extensive N–H \cdots O and C–H \cdots O interactions (drawn as dashed lines) linking the molecules into a complex three-dimensional array.

are bifurcated C–H \cdots O interactions involving O2 with graph-set notation $R_2^1(5)$. These interactions, along with C–H \cdots O interactions involving O4, link the molecules into a complex three-dimensional array.

4. Database survey

A search of the Cambridge Structural Database (CSD version 5.39; Groom *et al.*, 2016) using a skeleton containing the three rings as in thalidomide but without the ketone substituents gave 39 hits but not a single example where the six-membered aromatic ring in the isoindoline moiety is changed to an unsaturated six-membered ring.

5. Synthesis and crystallization

Some details of the synthesis have been previously reported (Benjamin & Hijji, 2017). *cis*-1,2-Cyclohexane dicarboxylic acid anhydride (0.10 g, 0.65 mmol), glutamic acid (0.095 g, 0.65 mmol), DMAP (0.02 g, 0.16 mmol), and ammonium chloride (NH₄Cl) (0.040 g, 0.75 mmol) were mixed thoroughly in a CEM-sealed vial with a magnetic stirrer. The sample was heated for 6 min at 423 K in a CEM Discover microwave powered at 150 W. It was then cooled rapidly to 313 K and dissolved in 15 ml of (1:1) ethyl acetate:acetone. The organic layer was washed with 2×10 ml of distilled water and dried over sodium sulfate (anhydrous). The organic layer was concentrated under vacuum and precipitated with hexanes (30 ml) affording a white solid. Crystals suitable for X-ray experiments were grown by slow evaporation of an ethyl acetate/acetone (1:1) solution. M.p. 463–465 K, (0.12 g, 70%). ¹H NMR (400 MHz, DMSO-*d*₆) δ 11.0 (*s*, 1 H, NH), 4.9 (*dd*, 1 H, 12.5, 5.5 Hz, CHCO), 3.0 (*m*, 1 H), 2.8 (*m*, 1 H), 2.8 (*m*, 1 H), 2.5 (*m*, 1 H), 1.9 (*m*, 1 H), 1.7 (*m*, 3 H), 1.6 (*m*, 1 H), 1.4 (*m*, 4 H); ¹³C NMR (100 MHz, DMSO-*d*₆) 178.8 (C=O), 178.7 (C=O), 172.7 (C=O), 169.4 (C=O), 48.7 (CH), 39.1 (CH), 38.8 (CH), 30.7 (CH₂), 23.1 (CH₂), 22.9 (CH₂), 21.1 (CH₂), 21.05 (CH₂), 21.00 (CH₂); MS 264 (M^+); 236, 210, 179, 154, 112, 82, 67, 54, 41.

6. Refinement

Crystal data, data collection and structure refinement details are summarized in Table 2. H atoms were positioned geometrically and treated as riding on their parent atoms and refined with C–H distances of 0.99–1.00 Å and $U_{\text{iso}}(\text{H}) = 1.2U_{\text{eq}}(\text{C})$. The H attached to N2 was refined isotropically. There is pseudomerohedral twinning present, which results from a 180° rotation about the [100] reciprocal lattice direction and with a twin law of 1 0 0 0 $\bar{1}$ 0 0 0 $\bar{1}$ [BASF 0.044 (1)].

Funding information

This report was made possible by a NPRP award [NPRP-7-495-1-094] from Qatar National Research Fund (a member of The Qatar Foundation). The statements made herein are solely the responsibility of the authors. RJB is grateful for the

Table 2
Experimental details.

Crystal data	
Chemical formula	C ₁₃ H ₁₆ N ₂ O ₄
<i>M_r</i>	264.28
Crystal system, space group	Monoclinic, <i>P</i> ₂ ₁ / <i>c</i>
Temperature (K)	123
<i>a</i> , <i>b</i> , <i>c</i> (Å)	11.4519 (3), 9.2370 (3), 11.8727 (4)
β (°)	90.475 (3)
<i>V</i> (Å ³)	1255.87 (7)
<i>Z</i>	4
Radiation type	Cu <i>K</i> α
μ (mm ⁻¹)	0.87
Crystal size (mm)	0.42 × 0.34 × 0.18
Data collection	
Diffractometer	Rigaku Oxford Diffraction Xcalibur, Ruby, Gemini
Absorption correction	Multi-scan (<i>CrysAlis PRO</i> ; Rigaku OD, 2012)
<i>T_{min}</i> , <i>T_{max}</i>	0.822, 1.000
No. of measured, independent and observed [<i>I</i> > 2 σ (<i>I</i>)] reflections	9733, 2626, 2572
<i>R_{int}</i>	0.024
(<i>sin</i> θ / λ) _{max} (Å ⁻¹)	0.633
Refinement	
<i>R</i> [<i>F</i> ² > 2 σ (<i>F</i> ²)], <i>wR</i> (<i>F</i> ²), <i>S</i>	0.066, 0.208, 1.19
No. of reflections	2626
No. of parameters	177
H-atom treatment	H atoms treated by a mixture of independent and constrained refinement
$\Delta\rho_{\max}$, $\Delta\rho_{\min}$ (e Å ⁻³)	0.33, -0.35

Computer programs: *CrysAlis PRO* (Rigaku OD, 2012), *SHELXS97* and *SHELXTL* (Sheldrick, 2008) and *SHELXL2018/3* (Sheldrick, 2015).

NSF award 1205608, Partnership for Reduced Dimensional Materials, for partial funding of this research as well as the Howard University Nanoscience Facility access to liquid nitrogen. RJB also acknowledges the NSF MRI program (grant No. CHE-0619278) for funds to purchase an X-ray diffractometer.

References

Allen, F. H. & Trotter, J. (1971). *J. Chem. Soc. B*, pp. 1073–1079.
 Bartlett, J. B., Dredge, K. & Dalglish, A. G. (2004). *Nat. Rev. Cancer*, **4**, 314–322.
 Begna, K., Pardanani, A., Mesa, R., Litzow, M., Hogan, W., Hanson, C. & Tefferi, A. (2012). *Am. J. Hematol.* **87**, 66–68.
 Benjamin, E. & Hijji, Y. M. (2017). *J. Chem.* pp. 1–6.
 Blaschke, G., Kraft, H. P., Fickentscher, K. & Köhler, F. (1979). *Arzneim.-Forsch.* **29**, 1640–1642.
 Boeyens, J. C. A. (1978). *J. Cryst. Mol. Struct.* **8**, 317–320.
 Brennen, W. N., Cooper, C. R., Capitosi, S., Brown, M. L. & Sikes, R. A. (2004). *Clin. Prostate Cancer*, **3**, 54–61.
 Burley, D. M. & Lenz, W. (1962). *Lancet*, **279**, 271–272.
 Cairra, M. R., Botha, S. A. & Flanagan, D. R. (1994). *J. Chem. Crystallogr.* **24**, 95–99.
 D'Amato, R. J., Loughnan, M. S., Flynn, E. & Folkman, J. (1994). *Proc. Natl Acad. Sci. USA*, **91**, 4082–4085.
 Eigler, A., Sinha, B., Hartmann, G. & Endres, S. (1997). *Immunol. Today*, **18**, 487–492.

Etter, M. C., MacDonald, J. C. & Bernstein, J. (1990). *Acta Cryst.* **B46**, 256–262.
 Franks, M. E., Macpherson, G. R. & Figg, W. D. (2004). *Lancet*, **363**, 1802–1811.
 Galustian, C. & Dalglish, A. (2011). *Drugs Fut.* **36**, 741–750.
 Groom, C. R., Bruno, I. J., Lightfoot, M. P. & Ward, S. C. (2016). *Acta Cryst.* **B72**, 171–179.
 Hashimoto, Y. (2008). *Arch. Pharm. Chem. Life Sci.* **341**, 536–547.
 Hashimoto, Y., Tanatani, A., Nagasawa, K. & Miyachi, H. (2004). *Drugs Fut.* **29**, 383–391.
 Knobloch, J. & Rüther, U. (2008). *Cell Cycle*, **7**, 1121–1127.
 Knoche, B. & Blaschke, G. (1994). *J. Chromatogr. A*, **666**, 235–240.
 Kumar, S., Witzig, T. E. & Rajkumar, S. V. (2002). *J. Cell. Mol. Med.* **6**, 160–174.
 Kumar, S., Witzig, T. E. & Rajkumar, S. V. (2004). *J. Clin. Oncol.* **22**, 2477–2488.
 Lovell, F. M. (1970). *ACA Abstr. Papers (Winter)*, 30.
 Lovell, F. M. (1971). *ACA Abstr. Papers (Summer)*, 36.
 Luzzio, F. A. & Figg, W. D. (2004). *Expert Opin. Ther. Pat.* **14**, 215–229.
 Maeno, M., Tokunaga, E., Yamamoto, T., Suzuki, T., Ogino, Y., Ito, E., Shiro, M., Asahi, T. & Shibata, N. (2015). *Chem. Sci.* **6**, 1043–1048.
 Matthews, S. J. & McCoy, C. (2003). *Clin. Ther.* **25**, 342–395.
 Melchert, M. & List, A. (2007). *Int. J. Biochem. Cell Biol.* **39**, 1489–1499.
 Moreira, A. L., Sampaio, E. P., Zmuidzinas, Z., Frindt, P., Smith, K. A. & Kaplan, G. J. (1993). *Exp. Med.* **177**, 1675–1680.
 Muller, G., Chen, R., Huang, S.-Y., Corral, L., Wong, L., Patterson, R., Chen, Y., Kaplan, G. & Stirling, D. (1999). *Bioorg. Med. Chem. Lett.* **9**, 1625–1630.
 Nishimura, K., Hashimoto, Y. & Iwasaki, S. (1994). *Chem. Pharm. Bull.* **42**, 1157–1159.
 Raje, N. & Anderson, K. (1999). *N. Engl. J. Med.* **341**, 1606–1609.
 Rao, S. T., Westhof, E. & Sundaralingam, M. (1981). *Acta Cryst.* **A37**, 421–425.
 Reepmeyer, J. C., Rhodes, M. O., Cox, D. C. & Silverton, J. V. (1994). *J. Chem. Soc. Perkin Trans. 2*, pp. 2063–2067.
 Rigaku OD (2012). *CrysAlis PRO*. Rigaku Oxford Diffraction, Yarnton, England.
 Sampaio, E. P., Sarno, E. N., Galilly, R., Cohn, Z. A. & Kaplan, G. (1991). *J. Exp. Med.* **173**, 699–703.
 Schey, S. & Ramasamy, K. (2011). *Expert Opin. Investig. Drugs*, **20**, 691–700.
 Sheldrick, G. M. (2008). *Acta Cryst.* **A64**, 112–122.
 Sheldrick, G. M. (2015). *Acta Cryst.* **C71**, 3–8.
 Singhal, S., Mehta, J., Desikan, R., Ayers, D., Roberson, P., Eddlemon, P., Munshi, N., Anaissie, E., Wilson, C., Dhodapkar, M., Zeldis, J., Siegel, D., Crowley, J. & Barlogie, B. (1999). *N. Engl. J. Med.* **341**, 1565–1571.
 Sleijfer, S., Kruit, W. H. J. & Stoter, G. (2004). *Eur. J. Cancer*, **40**, 2377–2382.
 Stephans, T. D. (1988). *Teratology*, **38**, 229–239.
 Suzuki, T., Tanaka, M., Shiro, M., Shibata, N., Osaka, T. & Asahi, T. (2010). *Phase Transit.* **83**, 223–234.
 Tseng, S., Pak, G., Washenik, K., Pomeranz, M. K. & Shupack, J. L. (1996). *J. Am. Acad. Dermatol.* **35**, 969–979.
 Wnendt, S., Finkam, M., Winter, W., Ossig, J., Raabe, G. & Zwingenberger, K. (1996). *Chirality*, **8**, 390–396.
 Wu, J. J., Huang, D. B., Pang, K. R., Hsu, S. & Tyring, S. K. (2005). *Br. J. Dermatol.* **153**, 254–273.
 Zeldis, J., Knight, R., Hussein, M., Chopra, R. & Muller, G. (2011). *Ann. N. Y. Acad. Sci.* **1222**, 76–82.

supporting information

Acta Cryst. (2018). E74, 1595-1598 [https://doi.org/10.1107/S2056989018014317]

Crystal structure of the thalidomide analog (3aR*,7aS*)-2-(2,6-dioxopiperidin-3-yl)hexahydro-1H-isoindole-1,3(2H)-dione

Yousef Hijji, Ellis Benjamin, Jerry P. Jasinski and Ray J. Butcher

Computing details

Data collection: *CrysAlis PRO* (Rigaku OD, 2012); cell refinement: *CrysAlis PRO* (Rigaku OD, 2012); program(s) used to solve structure: *SHELXS97* (Sheldrick, 2008); program(s) used to refine structure: *SHELXL2018/3* (Sheldrick, 2015); molecular graphics: *SHELXTL* (Sheldrick, 2008); software used to prepare material for publication: *SHELXTL* (Sheldrick, 2008).

(3aR*,7aS*)-2-(2,6-Dioxopiperidin-3-yl)hexahydro-1H-isoindole-1,3(2H)-dione

Crystal data

C₁₃H₁₆N₂O₄
M_r = 264.28
 Monoclinic, *P*2₁/*c*
a = 11.4519 (3) Å
b = 9.2370 (3) Å
c = 11.8727 (4) Å
 β = 90.475 (3)°
V = 1255.87 (7) Å³
Z = 4

F(000) = 560
D_x = 1.398 Mg m⁻³
 Cu *K*α radiation, λ = 1.54178 Å
 Cell parameters from 7629 reflections
 θ = 3.7–77.3°
 μ = 0.87 mm⁻¹
T = 123 K
 Prism, colorless
 0.42 × 0.34 × 0.18 mm

Data collection

Rigaku Oxford Diffraction Xcalibur, Ruby,
 Gemini
 diffractometer
 Detector resolution: 10.5081 pixels mm⁻¹
 ω scans
 Absorption correction: multi-scan
 (CrysAlisPro; Rigaku OD, 2012)
T_{min} = 0.822, *T_{max}* = 1.000

9733 measured reflections
 2626 independent reflections
 2572 reflections with *I* > 2σ(*I*)
R_{int} = 0.024
 θ_{\max} = 77.5°, θ_{\min} = 3.7°
h = -9→14
k = -10→11
l = -14→14

Refinement

Refinement on *F*²
 Least-squares matrix: full
R[*F*² > 2σ(*F*²)] = 0.066
wR(*F*²) = 0.208
S = 1.19
 2626 reflections
 177 parameters
 0 restraints
 Primary atom site location: structure-invariant
 direct methods

Secondary atom site location: difference Fourier
 map
 Hydrogen site location: mixed
 H atoms treated by a mixture of independent
 and constrained refinement
 $w = 1/[\sigma^2(F_o^2) + (0.1179P)^2 + 1.1244P]$
 where $P = (F_o^2 + 2F_c^2)/3$
 $(\Delta/\sigma)_{\max} < 0.001$
 $\Delta\rho_{\max} = 0.33 \text{ e \AA}^{-3}$
 $\Delta\rho_{\min} = -0.35 \text{ e \AA}^{-3}$

Special details

Geometry. All esds (except the esd in the dihedral angle between two l.s. planes) are estimated using the full covariance matrix. The cell esds are taken into account individually in the estimation of esds in distances, angles and torsion angles; correlations between esds in cell parameters are only used when they are defined by crystal symmetry. An approximate (isotropic) treatment of cell esds is used for estimating esds involving l.s. planes.

Refinement. Refined as a two-component twin

Fractional atomic coordinates and isotropic or equivalent isotropic displacement parameters (\AA^2)

	<i>x</i>	<i>y</i>	<i>z</i>	$U_{\text{iso}}^*/U_{\text{eq}}$
O1	0.66960 (17)	0.4309 (2)	0.56402 (17)	0.0291 (4)
O2	0.67111 (18)	0.8499 (2)	0.76606 (18)	0.0305 (5)
O3	0.58392 (17)	0.8448 (2)	0.51862 (17)	0.0299 (5)
O4	0.21720 (17)	0.9000 (2)	0.64578 (19)	0.0339 (5)
N1	0.64254 (19)	0.6373 (2)	0.66901 (18)	0.0228 (5)
N2	0.4008 (2)	0.8685 (2)	0.58537 (19)	0.0263 (5)
H2N	0.393 (4)	0.952 (5)	0.550 (3)	0.043 (10)*
C1	0.7100 (2)	0.5317 (3)	0.6160 (2)	0.0233 (5)
C2	0.8368 (2)	0.5762 (3)	0.6283 (2)	0.0240 (5)
H2A	0.886927	0.491448	0.648892	0.029*
C3	0.8713 (2)	0.6388 (3)	0.5124 (2)	0.0288 (6)
H3A	0.893112	0.558146	0.461791	0.035*
H3B	0.802837	0.688401	0.478581	0.035*
C4	0.9729 (2)	0.7454 (3)	0.5201 (2)	0.0311 (6)
H4A	1.043151	0.695475	0.549779	0.037*
H4B	0.990952	0.783222	0.444218	0.037*
C5	0.9407 (2)	0.8704 (3)	0.5979 (2)	0.0295 (6)
H5A	1.003226	0.944367	0.597275	0.035*
H5B	0.867389	0.916344	0.571200	0.035*
C6	0.9248 (2)	0.8128 (3)	0.7171 (2)	0.0278 (6)
H6A	0.899178	0.893048	0.766341	0.033*
H6B	1.001037	0.777727	0.746054	0.033*
C7	0.8356 (2)	0.6895 (3)	0.7240 (2)	0.0236 (5)
H7A	0.850009	0.636936	0.796398	0.028*
C8	0.7103 (2)	0.7412 (3)	0.7241 (2)	0.0235 (5)
C9	0.5186 (2)	0.6584 (3)	0.6460 (2)	0.0236 (5)
H9A	0.491323	0.576348	0.597625	0.028*
C10	0.5061 (2)	0.7980 (3)	0.5776 (2)	0.0239 (5)
C11	0.3047 (2)	0.8261 (3)	0.6481 (2)	0.0264 (5)
C12	0.3171 (2)	0.6889 (3)	0.7153 (2)	0.0285 (6)
H12A	0.288711	0.606388	0.669460	0.034*
H12B	0.267804	0.695498	0.783153	0.034*
C13	0.4435 (2)	0.6608 (3)	0.7512 (2)	0.0260 (5)
H13A	0.470638	0.737979	0.802975	0.031*
H13B	0.449314	0.566826	0.790999	0.031*

Atomic displacement parameters (\AA^2)

	U^{11}	U^{22}	U^{33}	U^{12}	U^{13}	U^{23}
O1	0.0298 (9)	0.0199 (9)	0.0374 (10)	-0.0011 (7)	-0.0051 (8)	-0.0043 (7)
O2	0.0306 (10)	0.0200 (9)	0.0407 (11)	0.0001 (7)	-0.0028 (8)	-0.0059 (7)
O3	0.0280 (10)	0.0269 (10)	0.0347 (10)	0.0042 (7)	0.0006 (8)	0.0055 (7)
O4	0.0266 (9)	0.0273 (10)	0.0478 (12)	0.0052 (8)	-0.0031 (8)	-0.0019 (9)
N1	0.0226 (10)	0.0164 (9)	0.0294 (10)	0.0004 (8)	-0.0062 (8)	0.0003 (8)
N2	0.0260 (11)	0.0189 (10)	0.0337 (11)	0.0043 (8)	-0.0044 (9)	0.0023 (9)
C1	0.0265 (12)	0.0173 (11)	0.0259 (11)	0.0017 (9)	-0.0049 (9)	0.0024 (9)
C2	0.0245 (11)	0.0177 (11)	0.0297 (12)	0.0005 (9)	-0.0039 (9)	0.0002 (9)
C3	0.0297 (13)	0.0276 (13)	0.0291 (13)	-0.0027 (10)	-0.0008 (10)	-0.0019 (10)
C4	0.0306 (13)	0.0319 (14)	0.0309 (13)	-0.0046 (11)	-0.0008 (10)	0.0011 (10)
C5	0.0286 (13)	0.0252 (13)	0.0345 (14)	-0.0050 (10)	-0.0035 (10)	0.0027 (10)
C6	0.0250 (12)	0.0275 (12)	0.0309 (13)	-0.0053 (10)	-0.0045 (10)	-0.0006 (10)
C7	0.0240 (11)	0.0216 (11)	0.0253 (11)	-0.0020 (9)	-0.0039 (9)	0.0014 (9)
C8	0.0250 (11)	0.0195 (11)	0.0258 (11)	-0.0010 (9)	-0.0043 (9)	0.0017 (9)
C9	0.0219 (11)	0.0170 (11)	0.0319 (12)	0.0015 (8)	-0.0070 (9)	-0.0005 (9)
C10	0.0253 (11)	0.0180 (11)	0.0283 (11)	0.0021 (9)	-0.0054 (9)	-0.0006 (9)
C11	0.0242 (12)	0.0213 (12)	0.0336 (13)	0.0007 (9)	-0.0054 (10)	-0.0053 (10)
C12	0.0245 (12)	0.0217 (12)	0.0393 (14)	-0.0016 (9)	-0.0017 (10)	0.0001 (10)
C13	0.0239 (12)	0.0218 (12)	0.0322 (13)	-0.0007 (9)	-0.0034 (10)	0.0030 (9)

Geometric parameters (\AA , $^\circ$)

O1—C1	1.207 (3)	C4—H4B	0.9900
O2—C8	1.208 (3)	C5—C6	1.525 (4)
O3—C10	1.217 (3)	C5—H5A	0.9900
O4—C11	1.213 (3)	C5—H5B	0.9900
N1—C8	1.394 (3)	C6—C7	1.532 (3)
N1—C1	1.397 (3)	C6—H6A	0.9900
N1—C9	1.456 (3)	C6—H6B	0.9900
N2—C10	1.374 (3)	C7—C8	1.513 (3)
N2—C11	1.390 (4)	C7—H7A	1.0000
N2—H2N	0.88 (5)	C9—C13	1.522 (4)
C1—C2	1.515 (3)	C9—C10	1.531 (3)
C2—C7	1.544 (3)	C9—H9A	1.0000
C2—C3	1.548 (4)	C11—C12	1.503 (4)
C2—H2A	1.0000	C12—C13	1.528 (4)
C3—C4	1.527 (4)	C12—H12A	0.9900
C3—H3A	0.9900	C12—H12B	0.9900
C3—H3B	0.9900	C13—H13A	0.9900
C4—C5	1.525 (4)	C13—H13B	0.9900
C4—H4A	0.9900		
C8—N1—C1	112.6 (2)	C5—C6—H6B	108.9
C8—N1—C9	122.3 (2)	C7—C6—H6B	108.9
C1—N1—C9	123.4 (2)	H6A—C6—H6B	107.8

C10—N2—C11	127.0 (2)	C8—C7—C6	113.4 (2)
C10—N2—H2N	118 (3)	C8—C7—C2	103.24 (19)
C11—N2—H2N	115 (3)	C6—C7—C2	117.1 (2)
O1—C1—N1	123.9 (2)	C8—C7—H7A	107.5
O1—C1—C2	128.4 (2)	C6—C7—H7A	107.5
N1—C1—C2	107.5 (2)	C2—C7—H7A	107.5
C1—C2—C7	103.9 (2)	O2—C8—N1	123.9 (2)
C1—C2—C3	105.49 (19)	O2—C8—C7	128.2 (2)
C7—C2—C3	113.9 (2)	N1—C8—C7	107.8 (2)
C1—C2—H2A	111.1	N1—C9—C13	113.9 (2)
C7—C2—H2A	111.1	N1—C9—C10	107.4 (2)
C3—C2—H2A	111.1	C13—C9—C10	111.9 (2)
C4—C3—C2	112.8 (2)	N1—C9—H9A	107.8
C4—C3—H3A	109.0	C13—C9—H9A	107.8
C2—C3—H3A	109.0	C10—C9—H9A	107.8
C4—C3—H3B	109.0	O3—C10—N2	121.2 (2)
C2—C3—H3B	109.0	O3—C10—C9	122.6 (2)
H3A—C3—H3B	107.8	N2—C10—C9	116.2 (2)
C5—C4—C3	109.7 (2)	O4—C11—N2	119.1 (2)
C5—C4—H4A	109.7	O4—C11—C12	124.1 (3)
C3—C4—H4A	109.7	N2—C11—C12	116.8 (2)
C5—C4—H4B	109.7	C11—C12—C13	112.1 (2)
C3—C4—H4B	109.7	C11—C12—H12A	109.2
H4A—C4—H4B	108.2	C13—C12—H12A	109.2
C6—C5—C4	109.2 (2)	C11—C12—H12B	109.2
C6—C5—H5A	109.8	C13—C12—H12B	109.2
C4—C5—H5A	109.8	H12A—C12—H12B	107.9
C6—C5—H5B	109.8	C9—C13—C12	108.3 (2)
C4—C5—H5B	109.8	C9—C13—H13A	110.0
H5A—C5—H5B	108.3	C12—C13—H13A	110.0
C5—C6—C7	113.2 (2)	C9—C13—H13B	110.0
C5—C6—H6A	108.9	C12—C13—H13B	110.0
C7—C6—H6A	108.9	H13A—C13—H13B	108.4
C8—N1—C1—O1	179.5 (2)	C9—N1—C8—C7	-174.9 (2)
C9—N1—C1—O1	-15.2 (4)	C6—C7—C8—O2	-34.8 (4)
C8—N1—C1—C2	-5.3 (3)	C2—C7—C8—O2	-162.5 (3)
C9—N1—C1—C2	160.0 (2)	C6—C7—C8—N1	147.1 (2)
O1—C1—C2—C7	-167.9 (2)	C2—C7—C8—N1	19.4 (3)
N1—C1—C2—C7	17.2 (2)	C8—N1—C9—C13	-67.6 (3)
O1—C1—C2—C3	72.0 (3)	C1—N1—C9—C13	128.4 (2)
N1—C1—C2—C3	-102.9 (2)	C8—N1—C9—C10	56.9 (3)
C1—C2—C3—C4	155.2 (2)	C1—N1—C9—C10	-107.1 (3)
C7—C2—C3—C4	41.9 (3)	C11—N2—C10—O3	179.1 (2)
C2—C3—C4—C5	-58.7 (3)	C11—N2—C10—C9	-0.4 (4)
C3—C4—C5—C6	64.9 (3)	N1—C9—C10—O3	25.9 (3)
C4—C5—C6—C7	-55.2 (3)	C13—C9—C10—O3	151.6 (2)
C5—C6—C7—C8	-80.1 (3)	N1—C9—C10—N2	-154.6 (2)

C5—C6—C7—C2	40.0 (3)	C13—C9—C10—N2	-28.9 (3)
C1—C2—C7—C8	-21.7 (2)	C10—N2—C11—O4	-179.6 (2)
C3—C2—C7—C8	92.6 (2)	C10—N2—C11—C12	0.4 (4)
C1—C2—C7—C6	-147.1 (2)	O4—C11—C12—C13	-151.1 (3)
C3—C2—C7—C6	-32.8 (3)	N2—C11—C12—C13	28.9 (3)
C1—N1—C8—O2	172.5 (2)	N1—C9—C13—C12	178.0 (2)
C9—N1—C8—O2	6.9 (4)	C10—C9—C13—C12	55.9 (3)
C1—N1—C8—C7	-9.4 (3)	C11—C12—C13—C9	-56.1 (3)

Hydrogen-bond geometry (Å, °)

<i>D</i> —H \cdots <i>A</i>	<i>D</i> —H	H \cdots <i>A</i>	<i>D</i> \cdots <i>A</i>	<i>D</i> —H \cdots <i>A</i>
N2—H2N \cdots O3 ⁱ	0.88 (5)	2.07 (5)	2.928 (3)	165 (4)
C7—H7A \cdots O4 ⁱⁱ	1.00	2.42	3.150 (3)	129
C9—H9A \cdots O1 ⁱⁱⁱ	1.00	2.65	3.385 (3)	130
C12—H12A \cdots O2 ⁱⁱ	0.99	2.53	3.143 (3)	120
C13—H13A \cdots O2	0.99	2.56	3.142 (3)	118
C13—H13B \cdots O2 ⁱⁱ	0.99	2.52	3.163 (3)	122

Symmetry codes: (i) $-x+1, -y+2, -z+1$; (ii) $-x+1, y-1/2, -z+3/2$; (iii) $-x+1, -y+1, -z+1$.